



PERGAMON

www.elsevier.com/locate/watres

Wat. Res. Vol. 35, No. 10, pp. 2460–2474, 2001
© 2001 Elsevier Science Ltd. All rights reserved
Printed in Great Britain
0043-1354/01/\$ - see front matter

PII: S0043-1354(00)00541-8

SIMPLIFIED ANALYSIS OF CONTAMINANT REJECTION DURING GROUND- AND SURFACE WATER NANOFILTRATION UNDER THE INFORMATION COLLECTION RULE

SHANKARARAMAN CHELLAM^{1*} and JAMES S. TAYLOR²

¹Department of Civil and Environmental Engineering, Cullen College of Engineering, University of Houston, 4800 Calhoun Road, Houston, TX 77204-4791, USA and ²Department of Civil Engineering, University of Central Florida, Orlando, FL 32816, USA

(First received 1 March 2000; accepted in revised form 1 October 2000)

Abstract—A simple, closed-form analytical expression based on the homogenous solution diffusion model is derived for contaminant removal during nanofiltration (NF) of ground and surface water. Solute permeation and back-diffusion coefficients were used as fitting parameters to model rejection characteristics of four thin-film composite NF membranes under conditions typical of drinking water NF. Nonlinear fits of the model to experimental data suggests that the United States Environmental Protection Agency's (USEPA)'s Information Collection Rule protocol for bench-scale studies could be improved to obtain greater precision of the mass transfer coefficients. The model was found to fit rejection data for several water treatment contaminants including total organic carbon, precursors to total organic halide, four trihalomethanes and nine haloacetic acids containing chlorine and bromine, calcium and total hardness, alkalinity and conductivity. The simplified approach to mass transfer calculations from multi-solute systems suggests that feed water recovery has a stronger influence on contaminant rejection than permeate flux. Evidence for coupled transport of divalent inorganic ions is also presented. Even though the model developed does not account for ion coupling and cannot be applied in a purely predictive mode, it can assist in the better design and interpretation of data obtained from site-specific pilot-scale water treatment NF studies conducted in support of plant design. © 2001 Elsevier Science Ltd. All rights reserved

Key words—nanofiltration, diffusive transport, water treatment, disinfection by-products, trihalomethanes, haloacetic acids, information collection rule, membrane filtration, non-linear regression

INTRODUCTION

Nanofiltration (NF) membranes typically operate at pressures less than 100 psi and are capable of high rejections of natural organic matter (NOM) and precursors to disinfection by-products (DBP) including trihalomethanes (THMs) and haloacetic acids (HAAs) (Tan and Amy, 1991; Blau *et al.*, 1992; Allgeier and Summers, 1995; Chellam, 2000), many of which are suspected carcinogens, mutagens, or teratogens. NF permeate water quality in multi-solute systems typical of water treatment applications is a complex function of physicochemical (steric and electrostatic) interactions between the membrane and dissolved solutes and many other factors that influence the solubility and diffusivity of solutes and

water in the membrane phase (Soltanieh and Gill, 1981). Even though many attempts have been made to describe solute transport across NF membranes from first principles, models are not available yet to accurately predict rejection from multi-component systems. This is due in part to complications arising from the need to preserve electroneutrality, ion pairing and coupling (Marinas and Selleck, 1992), and changes in diffusivity and viscosity in mixed solute systems.

One method of modeling ion coupling in multi-solute systems involves relating the separation data for a reference electrolyte such as NaCl to the target solute under consideration (Matsuura, 1993). At the heart of this approach is the measurement of a parameter $(-\Delta\Delta G/RT)_{\text{ion}}$ that is interpreted as the free energy required to bring the ion from the bulk solution to the inter-phase region of the membrane. In principle, if $(-\Delta\Delta G/RT)_{\text{ion}}$ values for all species in solution are known along with their diffusion and

*Author to whom all correspondence should be addressed.
Tel.: +713-743-4265; fax: +713-743-4260; e-mail: chellam@uh.edu

dissociation data at a fixed temperature, it will be possible to calculate solute permeability in multi-component systems. However, in most applications the complete feed water composition is not known. Additionally, thermodynamic properties of NOM cannot be well estimated because it is heterogeneous and does not possess a well-defined chemical and structural formula. For these reasons, a useful free energy based model may never be developed for NOM removal during water treatment. Therefore, our current approach to determining NF selectivity to NOM, DBP precursors, and inorganic ions in multi-component systems is largely empirical and is based on site-specific experiments (Tan and Amy, 1991; Blau *et al.*, 1992; Allgeier and Summers, 1995; Chellam *et al.*, 1997).

In order to better protect public health, the US Environmental Protection Agency (EPA) is facilitating regulatory negotiations to possibly reduce maximum contaminant levels (MCLs) of total THMs[†] (TTHMs), HAA5[‡], and possibly introduce new ones for HAA9[§], total organic halide (TOX) and even individual THM and HAA species under the Disinfectant/DBP (D/DBP) rule (USEPA, 1998). Earlier regulatory negotiations to reach consensus on the control of microbial contaminants and DBPs in drinking water resulted in the promulgation of the Information Collection Rule (ICR). The ICR required certain municipalities (based on population served and influent total organic carbon (TOC) concentration) to conduct experiments using NF or granular-activated carbon to better assess their feasibility to reduce DBP precursors under conditions close to those in a full-scale plant in terms of feed water quality and operational parameters (USEPA, 1996). This paper summarizes results from seven such crossflow NF ICR studies all of which appear to demonstrate diffusion-limited rejection of NOM, and THM, HAA, and TOX precursors. Most previous studies have not reported rejection of precursors to all nine HAAs containing chlorine and bromine by NF for because until recently stable calibration standards for dibromochloro-, dichlorobromo-, and tribromo acetic acid were not available.

Hindered transport across membrane pores controls the transport of single-neutral solutes across cellulose acetate NF membranes (Rosa and de Pinho, 1994). Molecular size correlates well with the retention of single-organic solutes by commercial NF membranes even though molecular charge and

polarity also influenced rejection (van der Bruggen *et al.*, 1999). In contrast to the single solutes of known properties employed in much previous research on organics separation by NF, NOM is inherently heterogeneous and possesses a wide distribution of molecular weight, aromaticity, functionality, hydrophobicity, and reactivity (Amy *et al.*, 1987; Chin *et al.*, 1994; Croue *et al.*, 1999). Additionally, membrane-NOM interactions depend on solution chemistry parameters including background ionic strength, pH, and concentrations of multivalent ions (e.g. Ca^{2+} , Al^{3+} , Fe^{3+}) (Hong and Elimelech, 1997; Cho *et al.*, 1999). Because complete chemical compositions of feed waters are often not available and since NOM is inherently heterogeneous, models based on NOM and membrane thermodynamic properties may never accurately predict its rejection from natural and pretreated waters by NF. We circumvent some of these difficulties by taking a lumped parameter approach to mass transfer calculations from multi-solute systems encountered during water treatment.

Previous NF studies on Florida groundwaters have suggested that physical sieving is the dominant mechanism for NOM and THM and HAA precursor rejection (Blau *et al.*, 1992). However, recent evidence appears to suggest that molecular diffusion also plays an important role in the transport of these contaminants across new generation thin film composite (TFC)-NF membranes formulated specifically for organics removal (Allgeier and Summers, 1995; Chellam, 2000). No models (including those developed by manufacturers themselves) currently exist to quantify rejection of NOM and DBP precursors by these membranes. Such a model will allow better design of pilot-scale experiments and more thorough interpretation of site-specific permeate water quality data from pilot studies conducted by municipalities to obtain design parameters for NF plants in anticipation of federal regulations establishing more stringent MCLs for THMs and HAAs.

We report results from ICR experiments that were designed to capture possible seasonal variations in feed water quality. We also develop and verify a simple closed form expression for contaminant rejection from several ground and surface waters based on the homogenous solution diffusion model (HSDM) (Lonsdale *et al.*, 1965) under conditions typical of water treatment NF applications using TFC membranes. Solute permeation and back-diffusion mass transfer coefficients are used to fit this model to rejection of several organic contaminants important in water treatment including TOC, ultraviolet absorption at 254 nm and 1 cm path length (UV_{254}), and precursors to TTHM, HAA9, and TOX. Rejection of selected inorganic water quality parameters such as alkalinity, total and calcium hardness, and conductivity are quantified. Coupled transport of divalent ions across NF membranes is also studied.

[†]TTHM denotes the sum of mass concentrations of chloroform, chlorodibromo methane, dichlorobromo methane, and bromoform.

[‡]HAA5 denotes the sum of mass concentrations of monochloro-, dichloro-, trichloro-, monobromo-, and dibromo acetic acid.

[§]HAA9 denotes the sum of HAA5 and mass concentrations of bromochloro-, dibromochloro-, dichlorobromo-, and tribromo acetic acid.

THEORETICAL WORK

Model development

Consider a NF system operating in the feed and bleed mode as shown in Fig. 1. In this configuration, a portion of the reject water is recirculated to maintain a predetermined tangential velocity (or shear rate) to limit concentration polarization. At steady state the volumetric water (J_w) and solute (J_s) fluxes when transport is diffusion-dominated and coupling is negligible (assuming constant membrane properties and diffusivity) is (Lonsdale *et al.*, 1965; Soltanieh and Gill, 1981; Matsuura, 1993; Taylor and Jacobs, 1996)

$$J_w = k_w \Delta P = \frac{Q_p}{A} \quad (1)$$

$$J_s = k_s \Delta C = J_w C_p \quad (2)$$

where k_w , k_s , Q_p and C_p represent a membrane constant, solute permeation coefficient, permeate flow, and permeate concentration, respectively. ΔP and ΔC are the driving forces for water and solute transport and are equal to net pressure (including osmotic pressure) and concentration differential between the membrane and permeate values. Fundamentally, the membrane constant k_w is related to the water diffusion coefficient in the polymeric membrane phase D_w , its concentration in the membrane c_w , its partial molar volume v_w , the universal gas constant R , the absolute temperature T , and the membrane thickness Δx as (Lonsdale, 1979)

$$k_w = \frac{D_w c_w v_w}{RT \Delta x} \quad (3)$$

Similarly, the solute permeation coefficient is related to its diffusivity in the membrane D_s and its distribution (partition) coefficient K_s as

$$k_s = \frac{D_s K_s}{\Delta x} \quad (4)$$

Because many thermodynamic parameters in equations (3) and (4) are not known for commercial membranes, we treat k_w and k_s as lumped parameters and will estimate them from experimental permeate flux and solute rejection data. These equations were originally developed to model mass transfer of simple electrolytes and organics across non-porous membranes. However, its applicability for NOM rejection

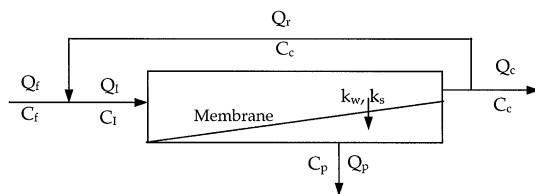


Fig. 1. Schematic diagram of a crossflow NF system operated in the feed and bleed mode.

by NF membranes especially in multi-solute systems has not yet been evaluated. The feed water (R_f) and element (R_e) recoveries are defined as

$$R_f = \frac{Q_p}{Q_f} \quad \text{and} \quad R_e = \frac{Q_p}{Q_f + Q_r} \quad (5)$$

where Q_f and Q_r denote the feed and recycle flows respectively. At steady state, a mass balance around the membrane module gives the reject concentration C_c :

$$C_c = \frac{C_f - R_f C_p}{1 - R_f} \quad (6)$$

Recycling part of the reject water to the feed side increases both the crossflow velocity as well as the influent concentration (C_1). At steady state, the influent concentration to the membrane is the flow-weighted average of the concentrations in the recycle and feed streams. Therefore, from equations (5) and (6) we get

$$C_1 = \left(\frac{R_e}{R_f} \right) C_f + \left(1 - \frac{R_e}{R_f} \right) \left(\frac{C_f - R_f C_p}{1 - R_f} \right) \quad (7)$$

The ratio C_1/C_f is interpreted as a concentration factor that $\rightarrow 1$ as $R_e \rightarrow R_f$ ($Q_r \rightarrow 0$). A simple one-dimensional description of concentration polarization based on film theory in which the net flux of solute in the boundary layer is equated to the flux through the membrane results in (Jonsson and Boesen, 1984; Matsuura, 1993; Taylor and Jacobs, 1996)

$$\frac{C_m - C_p}{C_b - C_p} = \exp\left(\frac{J_w}{k_b}\right) \quad (8)$$

where C_m is the concentration near the membrane surface, C_b is the bulk solution concentration, and k_b is the solute back-transport mass transfer coefficient. Approximating C_b as an arithmetic average of the influent and reject concentrations, the change in concentration across the membrane from equation (8) becomes

$$\Delta C = C_m - C_p = \left(\frac{C_1 + C_c}{2} - C_p \right) \exp\left(\frac{J_w}{k_b}\right) \quad (9)$$

Combining equations (1), (2), (7), and (9) a closed-form analytical expression for the solute rejection R is obtained

$$R = 1 - \frac{C_p}{C_f} = 1 - \frac{k_s \exp(J_w/k_b)}{k_s \exp(J_w/k_b) + 2J_w(1 - R_f)/(2 - R_e)} \quad (10)$$

Equation (10) represents a solute-mass transfer model for systems employing concentrate recycle that considers the entire membrane element as having constant bulk solution concentration calculated as the average of the influent and reject concentrations. Therefore, it represents an important approximation whose accuracy increases as the feed water recovery

decreases (so as to limit increases in C_b). However, invoking this approximation results in an analytical, closed form solution thereby lending itself to mechanistic interpretation of solute rejection data from multi-component feed waters obtained during municipal water treatment experiments conducted in support of plant design and/or trouble shooting. One method of calculating k_s and k_b is by using appropriate mass transfer correlations (van den Berg *et al.*, 1989). These empirical correlations are intimately linked to the geometry and type of spacer material used as well as the local hydrodynamics and typically do not include changes in viscosity and diffusivity caused by concentration polarization. Because spacer information is proprietary and hydrodynamic behavior in the presence of spacers are not well understood, k_s and k_b will be estimated from experimental data in this study as described in the next section.

Because the partial derivative of R with respect to R_f in equation (10) is always negative, it can be concluded that rejection will decrease with increasing recovery. Mechanistically, this occurs because of increasing concentration gradient thereby increasing the driving force for solute permeation across the membrane. This behavior will be employed predominantly to study solute rejection by NF membranes in this paper.

Parameter estimation

The Levenberg–Marquardt algorithm (Press *et al.*, 1992) was employed to minimize the sum of squares of the residuals for all data points (error sum of squares (S)) to determine k_s and k_b . Estimates for selected datasets were also verified using a more robust full Newton-type method to minimize the nonlinear sum of squares employing an analytical Jacobian (Dennis *et al.*, 1981). The joint $(1 - \alpha)$ likelihood region for k_s and k_b corresponds to the contour with level

$$S_F = S(\hat{\Theta}) \left[1 + \frac{pF(p, n-p, \alpha)}{n-p} \right] \quad (11)$$

where α is the significance level, S_F denotes the value of the sum of squares contour defining the $(1 - \alpha)$ region, S is the sum of squares of the residuals, $\hat{\Theta}$ denotes the optimal parameter estimate, p is the number of parameters ($p = 2$ in equation (10)), n is the number of observations, $F(p, n-p, \alpha)$ is the cumulative Fisher F distribution corresponding to significance level α with p and $n-p$ degrees of freedom for the numerator and denominator, respectively. Nonlinear nominal likelihood intervals and nonlinear behavior were quantified by profiling (Bates and Watts, 1988; Watts, 1994). The profile t function is defined as

$$\tau(\Theta_p) = \text{sign}(\Theta_p - \hat{\Theta}_p) \frac{\sqrt{S(\Theta_p) - S(\hat{\Theta})}}{s} \quad (12)$$

where Θ_p denotes a parameter, $\hat{\Theta}_p$ denotes the parameter's optimal value, S is the profile sum of squares function, and s^2 is the variance estimated as $S(\hat{\Theta})/(n-p)$. Plots of the profile t function τ vs. the studentized parameter δ (equation (13)) provide exact likelihood intervals for k_s and k_b :

$$\delta(\Theta_p) = \frac{\Theta_p - \hat{\Theta}_p}{\text{se}(\hat{\Theta}_p)} \quad (13)$$

where, $\text{se}(\hat{\Theta}_p)$ denotes the standard error of the least-squares estimate. Likelihood profile traces of \hat{k}_b on k_s and \hat{k}_s on k_b were also generated to determine the extent of nonlinearity in parameter estimation.

EXPERIMENTAL WORK

Nanofiltration experiments

Crossflow experiments were conducted in the feed and bleed mode using the protocol specified by USEPA for bench-scale ICR NF experiments (USEPA, 1996). For these studies, a pressurized cell using a flat membrane sheet was employed (model SEPA-CF, Osmonics, Minnetonka, MN). This cell utilized feed and permeate spacers (0.07 and 0.025 cm thick, respectively) that are also used in commercial spiral-wound elements. The use of positive displacement gear pumps for both feed water (Cole Palmer, Vernon Hills, IL model 74011-11) and recycle water (Cole Palmer, Vernon Hills, IL model 07002-23) minimized pressure fluctuations. These pumps employed helical gears made of inert, low-friction materials to reduce potential frictional losses on the gears. All tubing, connections, and the membrane cell were fabricated of stainless steel. Dual float rotameters increased the accuracy of the flow measurements. In addition, permeate and waste flows were manually measured using a graduated cylinder and a stopwatch.

Water samples were collected every three months in a one-year period to conduct seasonal NF experiments using two different membranes. Prior to experiments with the pretreated source water, deionized water was passed through the whole system for ~ 24 h prior to experiments with the test water. This period is sometimes referred to as membrane setting. All experiments were conducted at room temperature ($\sim 22^\circ\text{C}$). Therefore, any effects caused by seasonal variability in water temperature were not reflected in the data obtained. A pressure-flux profile was conducted prior to filtration of test water to determine the water permeation coefficient. During these measurements, the transmembrane pressure was changed in random order in the range 0–550 kPa (0–80 psi) and the flux measured at the set pressures. The transmembrane pressure was then adjusted to obtain an initial permeate flux of $\sim 25 \text{ L/m}^2/\text{h}$ ($\sim 15 \text{ gfd}$).

During each quarter, constant pressure experiments using pretreated source waters were conducted continuously with each membrane for a period of ~ 150 h. Feed water recovery for the first experiment was maintained at $\sim 70\%$ and was run for a minimum of 78 h. During this time, two 5 L permeate water samples were collected to perform duplicate water quality analyses. This was followed by experiments where recovery was maintained at values near 90, 50, and 30%, respectively. As required by the ICR, experiments at various recoveries were conducted without any membrane cleaning. Experiments at other recoveries were run for sufficient duration to collect a minimum of 4 L of permeate water to conduct all required analyses. Composite sampling began only after UV_{254} and conductivity reached a steady value in the permeate water (defined in this study as $< 3\%$ change in samples collected over the span of 1 h).

Source waters and NF pretreatment

Important characteristics of the four groundwaters and three surface waters employed in this study following pretreatment are summarized in Table 1. These data represent averages calculated from analyses conducted over the course of four quarters during a 12-month period. These feed waters represent a wide range of various organic and inorganic water quality parameters including TOC (2.9–13.1 mg/L), TTHM precursors (75–527 µg/L), HAA9 precursors (73–274 µg/L), total hardness (33–355 mg/L as CaCO₃), alkalinity (9–305 mg/L as CaCO₃) and conductivity (162–1370 µS/cm). Each participating utility sent ~350 L of water (collected prior to adding any oxidants or chemical disinfectants) to our laboratory during each quarter. The only NF pretreatment for the groundwaters was depth filtration using a 5 µm cartridge (Ryan Herco, Burbank, CA). Surface waters E, F, and G were coagulated and flocculated (using alum), settled (~3 h) and filtered using a 5 µm cartridge.

Membranes employed

Four manufacturer recommended TFC-NF membranes were selected to study NOM rejection. Important manufacturer specifications and rejections measured at 70% recovery during this study are summarized in Table 2. All membranes employed in this study are available commercially in spiral-wound geometry for larger scale applications. A new 155-cm² membrane coupon was used for each set of experiments with changing recovery.

Simulated distribution system testing

Removals of TTHM, HAA9, and TOX precursors were measured using simulated distribution system tests with free chlorine as required by the ICR. These tests simulated each participating utility's quarterly average of full-scale distribution system pH, temperature, and residence time (Table 3). During SDS testing, the sample water was dosed with sodium hypochlorite after pH adjustment in chlorine demand free bottles. These bottles were then held in the dark to obtain a free chlorine residual near 1 mg/L at the conclusion of the incubation period. Trial chlorine demand tests were conducted with at least two free chlorine dosages for both the feed and permeate water samples to determine appropriate dosages for actual SDS testing. SDS conditions varied with utility and in some cases with season. However, all comparisons of TTHM, HAA9, and TOX precursor removal by NF presented in this manuscript were made using data corresponding to the same SDS conditions. In other words, DBP precursor rejections were quantified under identical SDS conditions for the feed and permeate waters.

Analytical methods

Only standard methods (Clesceri *et al.*, 1998) or EPA approved methods (USEPA, 1996) with appropriate quality control procedures were used to quantify contaminant concentrations. Table 4 summarizes all methods employed and the minimum reporting level for each contaminant. At the conclusion of each SDS test, chlorine residual was measured using the DPD colorimetric method. TOC, THM, HAA, and TOX samples were then collected headspace free in amber-glass bottles and stored at ~4°C until analysis. Chlorine residuals were quenched using ammonium chloride, sodium thiosulfate, and sodium sulfite for HAA, THM, and TOX respectively. Both TOX and TOC samples were acidified to pH <2 using H₂SO₄ prior to analysis. Alkalinity and hardness concentrations were determined by burette titration. pH and conductivity were quantified using appropriate probes. UV₂₅₄ was measured using a 1-cm path length cell.

Table 1. Summary of source water locations and average membrane feed water quality

Designation	Source water	TOC conc. (mg/L)	UV ₂₅₄ (cm ⁻¹)	Br ⁻ conc. (µg/L)	SDSTTHM conc. (µg/L)	SDSHAA9 conc. (µg/L)	SDSTOX conc. (µg Cl ⁻ /L)	Total hardness conc. (mg/L as CaCO ₃)	Calcium hardness conc. (mg/L as CaCO ₃)	pH	Conductivity (µS/cm)	Alkalinity conc. (mg/L as CaCO ₃)	Membranes employed
A	Biscayne Aquifer, FL	12.1	0.417	154	342	274	1073	272	238	8.1	602	288	I, II
B	Biscayne Aquifer, FL	13.1	0.579	143	527	265	1374	252	223	8.1	594	291	I, II, III
C	Biscayne Aquifer, FL	6.35	0.187	127	205	75	544	282	253	8.0	446	305	I, II
D	Biscayne Aquifer, FL	4.01	0.150	75	135	73	351	250	227	7.8	530	268	I, II
E	Lake Meade, VA	3.3	0.053	42	75	81	276	33	25	6.5	162	8.6	I, IV
F	Caloosahatchee River, FL	7.1	0.154	186	252	191	890	201	158	7.5	536	116	I, II, III
G	Rio Grande River, TX	2.9	0.067	413	214	103	304	355	237	8.1	1370	155	I, II, III

Note: A, B, C, and D are ground waters. The only NF pretreatment for these waters was laboratory scale depth filtration using a 5 µm cartridge filter. E, F, and G are surface waters. Prior to NF, E and F were pretreated (coagulation and flocculation at full-scale and sedimentation (~3 h) and 5 µm cartridge filtration at bench-scale). G was pretreated using coagulation, flocculation, and sedimentation at bench-scale. The water quality parameters represent an average of quarterly measurements made during a one-year period on the membrane feed water i.e. following pretreatment. Membrane designations are given in Table 2.

Table 2. Summary of membranes employed and their rejection characteristics from pretreated waters

Parameter	Membrane characteristics			
	I	II	III	IV
Designation				
Manufacturer	Hydranautics, San Diego, CA	Koch Fluid Systems, San Diego, CA	Dow FilmTec, Midland, MI	Dow FilmTec, Midland, MI
Model number	NTR 7450	TFC-SR	NF 200B	NF45
Composition ^a	Modified polysulfone	Polyamide	Polypiperazine	Polyamide
MWCO (Dalton) ^a	600–800	300	200–400	400
Hydrophobicity ^a	Hydrophobic	NA ^b	Hydrophilic	Hydrophobic
Surface charge ^a	Negative	Slightly negative	Highly negative	Negative
Clean membrane constant (m/s/Pa) ^c	1.39×10^{-11}	1.84×10^{-11}	1.74×10^{-11}	1.39×10^{-11}
TOC rejection (%) ^d	71	94	91	93
UV ₂₅₄ rejection (%) ^d	80	97	93	94
TTHM precursor mass rejection (%) ^d	68	93	87	89
HAA9 precursor mass rejection (%) ^d	68	97	91	91
TOX precursor mass rejection (%) ^d	77	95	89	79
Bromide rejection (%) ^d	3	10	–3	10
Conductivity rejection (%) ^d	8	27	25	65
Calcium hardness rejection (%) ^d	15	42	50	93
Total hardness rejection (%) ^d	12	42	47	96
Alkalinity rejection (%) ^d	10	25	14	14

^aSpecified by the manufacturer. Surface charge reported at near neutral pH.

^bDenotes not available.

^cMedian of all measurements during this study.

^dMedian of all measurements at 70% recovery in this study.

Table 3. Summary of simulated distribution system conditions employed^a

Source water	Quarter	pH	Temperature (°C)	Holding time (h)
A	I-IV	8.0	24	24
B	I-IV	9.0	24	24
C	I-IV	9.0	24	24
D	I-IV	8.0	24	24
E	I	7.3	10	60
	II	7.3	18	60
	III	7.3	28	72
	IV	7.3	16	72
F	I	8.0	24	24
	II	8.0	24	48
	III	8.0	24	72
	IV	8.0	24	48
G	I	8.2	24	72
	II	8.2	24	48
	III	8.2	24	24
	IV	8.2	24	48

^aIn all cases free chlorine was the disinfectant with a target residual ~1 mg/L at the end of the holding period.

RESULTS AND DISCUSSION

Solute mass balances

Mass balances were conducted around the membrane cell for various contaminants after steady state was reached. Experimental reject water concentration data were compared to calculations using equation (6). Excellent agreement between experimental observations and theoretical calculations were noted in all cases. (Details of model fits using equation (10) to experimental data are provided in the Sections "Organics rejection" and "Inorganics rejection"). Additionally, two-sided, two sample *t*-tests also showed that there were no differences in the means of the calculated and measured concentrations at 95% confidence level. These mass balances show that the sampling protocol was acceptable, and the water quality analyses and flow measurements were accurate.

Membrane constant

Results from pressure-flux profiles were modeled using equation (1). Membranes II and III were more permeable to deionized water ($k_w \sim 1.82 \times 10^{-11}$ m/s/Pa) compared to membranes I and IV ($k_w \sim 1.39 \times 10^{-11}$ m/s/Pa). Additionally, in the pressure range employed (< 550 kPa) permeate flux increased linearly with transmembrane pressure for all four membranes suggesting that compaction effects were negligible under the conditions employed in this study.

Organics rejection

As shown in Table 1, rejection of TOC and precursors to TTHM, HAA9, and TOX were in the order membrane II > III \approx IV > I. Membrane I achieved > ~95% rejection; membranes III and IV achieved ~90% rejection whereas membrane I rejected only ~70% of these organic contaminants.

Table 4. Summary of Analytical methods and minimum reporting levels

Analyte	Method	Description	Minimum reporting level
TOC	SM 5310C	Persulfate-Ultraviolet oxidation	0.20 mg/L.
CHCl ₃ , BDCM, DBCM, CHBr ₃	EPA 502.2	Purge and trap capillary column gas chromatography with photoionization and electrolytic conductivity detectors	1 µg/L for each analyte.
CHCl ₃ , BDCM, DBCM, CHBr ₃	EPA 524.2	Capillary column gas chromatography/mass spectroscopy	1 µg/L for each analyte.
CHCl ₃ , BDCM, DBCM, CHBr ₃	EPA 551.1	Liquid-liquid extraction gas chromatography and electron-capture detection	1 µg/L for each analyte.
MCAA, DCAA, TCAA, MBAA, DBAA, TBAA, BCAA, BDCAA, DBCAA	SM 6251B	Micro liquid-liquid extraction gas chromatography	2,1,1,1,1,4,1,1, and 2 µg/L, respectively
MCAA, DCAA, TCAA, MBAA, DBAA, TBAA, BCAA, BDCAA, DBCAA	EPA 552.2	Liquid-liquid extraction, derivatization, and gas chromatography with electron capture detection	2,1,1,1,1,4,1,1, and 2 µg/L, respectively
TOX	SM 5320B	Adsorption-pyrolysis-titrimetry	20 µg Cl ⁻ /L
pH	SM 4500H+	Electrometric (probe) method	NA
Alkalinity	SM 2320B	H ₂ SO ₄ titration	10 mg/L as CaCO ₃
Calcium hardness	SM 2340C	Ethylenediaminetetraacetic acid titration	5 mg/L as CaCO ₃
Total hardness	SM 2340C	Ethylenediaminetetraacetic acid titration	10 mg/L as CaCO ₃
Bromide	EPA 300.0	Ion chromatography	20 µg/L
UV ₂₅₄	SM 5910B	Ultraviolet absorption at 254 nm	0.004 cm ⁻¹
Cl ₂ residual	SM 4500Cl	DPD Colorimetry at 530 nm	0.5 mg/L
Conductivity	SM 2510B	Conductivity probe	1 µS/cm

In general, HAA9 precursors were removed to a slightly greater extent than TTHM precursors.

Model calculations of HAA9 precursor rejection is depicted in Fig. 2 along with experimental measurements for source water *D* using membrane *I*. Good agreement between model calculations and laboratory data is observed ($S(\hat{\Theta})=0.179$). Similar results were obtained for other membrane—source water combinations for the range of organic water quality parameters investigated. A discussion of model parameter estimates is postponed until the Section “Behavior of parameter estimates”. Figure 2 shows that within the range of experimental conditions investigated in this study, HAA9 precursor removal is a strong function of feed water recovery but is only weakly influenced by permeate flux. Rejection decreases as recovery increases because concentration gradient across the membrane is increased. Rejection effectively increases with permeate flux according to the HSDM because increasing transmembrane pressure does not influence solute transport while increasing permeate flux (Sourirajan, 1970; Lonsdale, 1979; Wiesner and Buckley, 1996).

The effect of recovery on TOX precursor rejection from source water *F* is shown in Fig. 3(a) for membranes I–III at an average flux of 21.5 L/m²/h and 22°C and identical SDS conditions. The transport of TOX precursors across these membranes also appears to be influenced by molecular diffusion because their rejection decreases with increasing recovery. Interestingly, model parameters included in Fig. 3(a) show that the back-transport coefficient varied only in the narrow range 1.50–1.88 μm/s for all three membranes (average TOX $k_b=1.73$ μm/s). However, under the same conditions k_s varied over 14-fold from 0.002 to 0.028 μm/s. Increasing solute permeation coefficient manifests decreasing rejection with different membranes. Membrane II achieved

highest TOX precursor rejection ($k_s=0.002$ μm/s) whereas membrane I demonstrated lowest TOX precursor rejection ($k_s=0.028$ μm/s). Thus, k_s appears to be a very good descriptor of solute mass transfer across these TFC-NF membranes. Diffusive transport of TOX precursors was observed for other membrane—source water combinations also during the course of one year. One example is depicted in Fig. 3(b) where TOX precursor rejection from four sets of experiments conducted over the course of one year to evaluate seasonal changes in feed water quality are summarized. Decreasing rejection with increasing recovery during these replicate experiments appear to confirm the importance of molecular diffusion on TOX precursor removal by NF membranes. Even though similar observations have been made with monovalent (sodium) ion transport (Taylor and Jacobs, 1996) to our knowledge, these are amongst the first calculations of diffusion-dominated transport of DBP precursors across TFC-NF membranes during water treatment.

Inorganics rejection

As seen in Table 2, membranes I–III rejected NOM and DBP precursors to a much greater extent than the inorganic contaminants. Membrane IV rejected inorganics to a greater extent than membranes I–III. Total hardness will be used as a representative example in the discussions on inorganics rejection that follow next.

Model calculations of total hardness rejection is depicted in Fig. 4 along with experimental measurements for source water *G* using membrane III. Again, in the range of experimental parameters investigated, the feed water recovery strongly influenced hardness removal, whereas permeate flux had only a weak effect. Similar results were obtained for other membrane—source water combinations for the range of inorganic water quality parameters investigated as long as ion coupling was low (see next Section). Rejection decreased as recovery increased due to increasing concentration gradient across the membrane. As expected from the HSDM, rejection increased slightly as flux increased. Good agreement is seen between experimental observations and model calculations ($S(\hat{\Theta})=0.223$). A detailed discussion of model parameter fits to laboratory data is postponed until the Section “Behavior of parameter estimates”.

The role of molecular diffusion on the transport of ions contributing to total hardness across membranes I–III is depicted in Fig. 5(a) where increasing recovery (at a constant flux) is seen to decrease rejection. As before, k_b values remained in a narrow range [1.72–1.95 μm/s] (average $k_b=1.84$ μm/s) even with changing membrane type. Increasing k_s values manifested decreasing rejection. Membrane I achieved the lowest total hardness rejection from source water *F* ($k_s=0.33$ μm/s) whereas k_s decreased to 0.05 μm/s for membrane II that demonstrated the

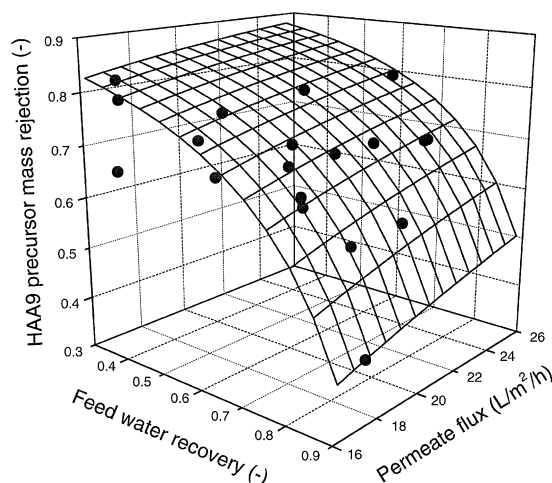


Fig. 2. Model calculations of HAA9 precursor removal from source water *D* by membrane *I*. Experimental data are superposed for comparison purposes. ($S(\hat{\Theta})=0.179$, $k_s=0.65$ μm/s, $k_b=130$ μm/s, $R_c=0.02$).

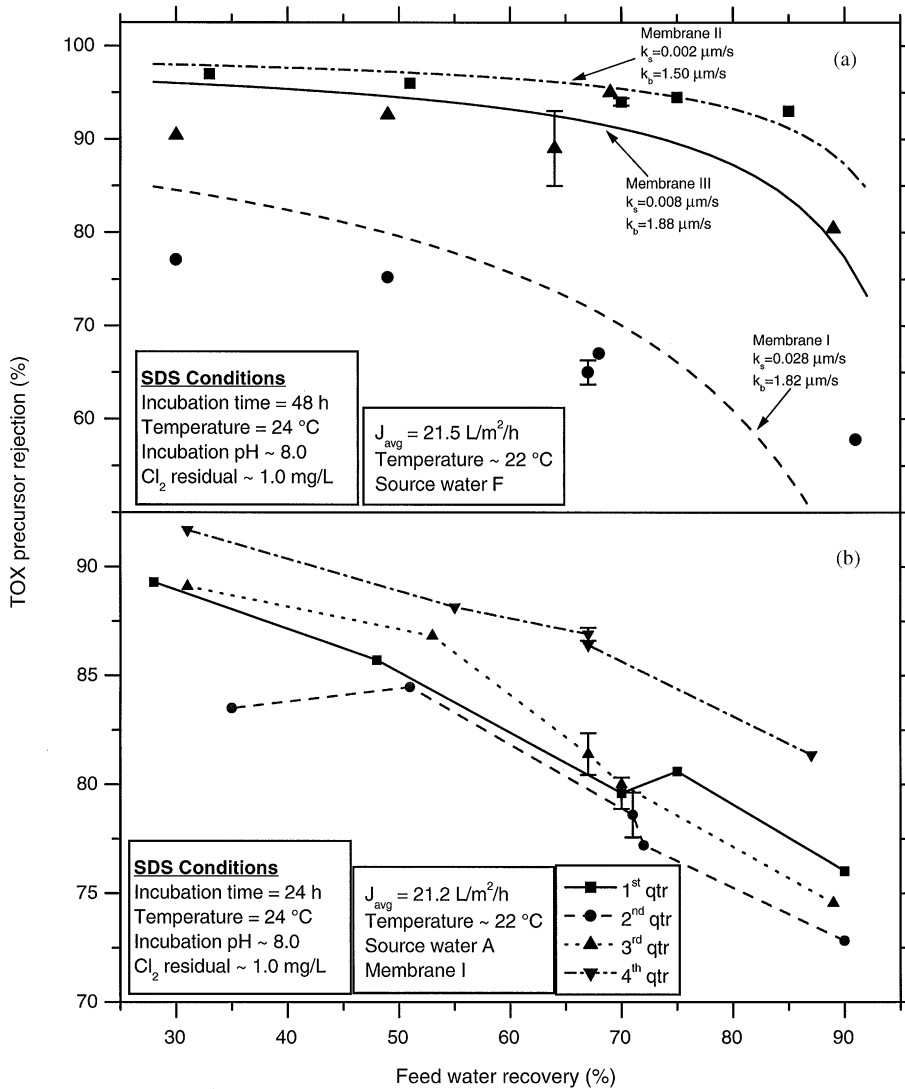


Fig. 3. Comparison of TOX precursor rejection by three NF membranes at various feed water recoveries for source water F (a). Theoretical fits are superposed on experimental observations for comparison. TOX precursor rejection for replicate experiments conducted over a one-year period with seasonal changes in feed water quality for source water A using membrane I are depicted in (b).

highest total hardness rejection. These results suggest that k_s is also a good descriptor of inorganic ion rejection by TFC-NF membranes during municipal water treatment. Replicate experiments conducted over the course of one year to assess impacts of seasonal variation in feed water quality confirm decreasing rejection with increasing recovery (Fig. 5(b)). Decreases in rejection with increases in recovery during the entire course of this study appear to confirm the importance of diffusive transport in the removal of hardness causing ions by the TFC polymeric membranes.

Ca⁺² and SO₄⁻² ion-coupling. Substantial changes in diffusion-limited rejection can be observed during NF of multi-component solutions because of electro-

neutrality considerations. For example, calcium ion selectivity for membranes II and III are depicted in Fig. 6 for source waters B and G. As seen from Table 1, the calcium hardness of these waters is similar (~ 230 mg/L as CaCO₃) whereas conductivity in source water G is \sim two times higher compared to source water B. Higher concentrations of SO₄⁻² were also measured in source water G (288 mg/L) compared to source water B (20 mg/L). Under these conditions, calcium ion rejection by both membranes decreased by a factor ~ 2 for all recovery values for source water B compared to source water G (see Fig. 6). For example, membrane II achieved $\sim 80\%$ rejection of calcium hardness from source water G but only $\sim 40\%$ from source water B at 50% recovery.

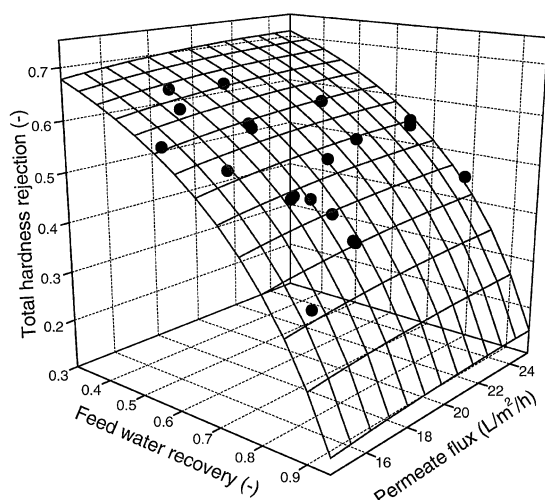


Fig. 4. Effects of permeate flux and feed-water recovery on total hardness removal from source water G by membrane III. Experimental data are superposed on model calculations for comparison purposes. ($S(\Theta) = 0.223$, $k_s = 0.79 \mu\text{m/s}$, $k_b = 7.54 \mu\text{m/s}$, $R_c = 0.02$).

These results are consistent with coupled transport of ions across these membranes from multi-solute feed waters in order to preserve electroneutrality (Marinas and Selleck, 1992; Taylor and Jacobs, 1996; Wiesner and Buckley, 1996). All membranes evaluated in this study are reported by respective manufacturers to be negatively charged at pH values employed (6.5–8.1). Other TFC-NF membranes have also been reported to be negatively charged at different solution chemistries encompassing this pH range (Childress and Elimelech, 1996). Electrostatic repulsion is the primary anion rejection mechanism by negatively charged membranes. Thus, increasing concentrations of highly rejected divalent anions such as SO_4^{2-} should simultaneously increase Ca^{+2} rejection because of the higher stability constants of 2–2 ion pairs (e.g. CaSO_4^0) compared to 1–1 (NaCl^0) or 2–1 (e.g. NaSO_4^- , Na_2SO_4^0) ion pairs (Martell and Motekaitis, 1992; Stumm and Morgan, 1996) so as to preserve electroneutrality in the feed stream. Such behavior should also concurrently decrease the rejection of monovalent ion pairs (e.g. NaCl^0 and NaHCO_3^0). As expected, alkalinity rejection for both membranes increased for source water B compared to source water G (data not shown). However, because monitoring for Na^+ and Cl^- was not required under the ICR their concentrations were not measured in these studies. These results demonstrate that softening and alkalinity removal capabilities of a given nanofilter should not be universalized as “high” or “low” without considering the complete feed water chemistry.

Model parameters shown in Fig. 6 again demonstrate that decreasing rejection for various membrane-source water combinations is manifested as increasing k_s values while k_b remains in a narrow

range [1.76–1.93 $\mu\text{m/s}$] (average $k_b = 1.88 \mu\text{m/s}$). A ~ 10 fold increase in k_s (from 0.02 to 0.23 $\mu\text{m/s}$) was calculated when calcium hardness rejection increased from $\sim 20\%$ for membrane III (source water B) to $\sim 80\%$ for membrane II (source water G) at 70% recovery. Ion coupling reduced the importance of feed water recovery on calcium removal. As seen in Fig. 6, rejection of calcium hardness from source water G appeared to be relatively constant with feed water recovery for both membrane II and III. This also resulted in poor model fits to experimental data. However, when SO_4^{2-} concentrations were low (and coupling was reduced), equation (10) was a better descriptor of calcium transport across these NF membranes.

Behavior of parameter estimates

Graphical summaries of nonlinear estimations of mass transfer coefficients and their inference regions are provided in Fig. 7 for four quarters of TOC removal from source water G using membrane III. Profile t plots (τ vs. δ) for k_b and k_s are shown in Fig. 7(a) and (b), respectively. The dashed straight line is the linear approximation of the joint parameter likelihood region. In all cases, the τ curves lie below the linear approximation line suggesting that the sum of squares of the residuals surface has a large negative slope (steep fall) as k_s and k_b values approach the least-squares estimate from the left and has a small positive slope (slow rise) as they increase beyond the optimal value (Watts, 1994).

All profile t plots for k_s and k_b are highly curved and even tend to asymptotes, indicating severe nonlinearity. Thus, the likelihood intervals are extremely skewed and asymmetric about the least-squares point estimate. Asymptotic behavior also results in likelihood intervals that do not close on the right (unbounded upper limit) above some significance level (Bates and Watts, 1988). For example, as seen in Fig. 7(a) and (b) the second quarter joint likelihood regions for both k_s and k_b do not close on the right (indeterminate upper limit) for significance levels of $\sim 50\%$.

Close agreement between experimental C_p/C_f ratios and theoretical calculations for all four quarters for TOC and total dissolved solids (TDS) are seen in Fig. 7(c) and (d), respectively. The average absolute deviation of theoretical predictions from experimental values was 24% for TOC and 8% for TDS. Simple two sided t -tests also showed that the averages of the experimental and theoretical values for all seasons were not statistically different at the 99% confidence level for both TOC and TDS suggesting that equation (10) is a good descriptor of both organic and inorganic contaminant rejection by NF membranes. However, point estimates were derived with poor precision as explained next.

Joint parameter likelihood regions around the least-squares estimate ($k_s = 0.023 \mu\text{m/s}$, $k_b = 2.21$

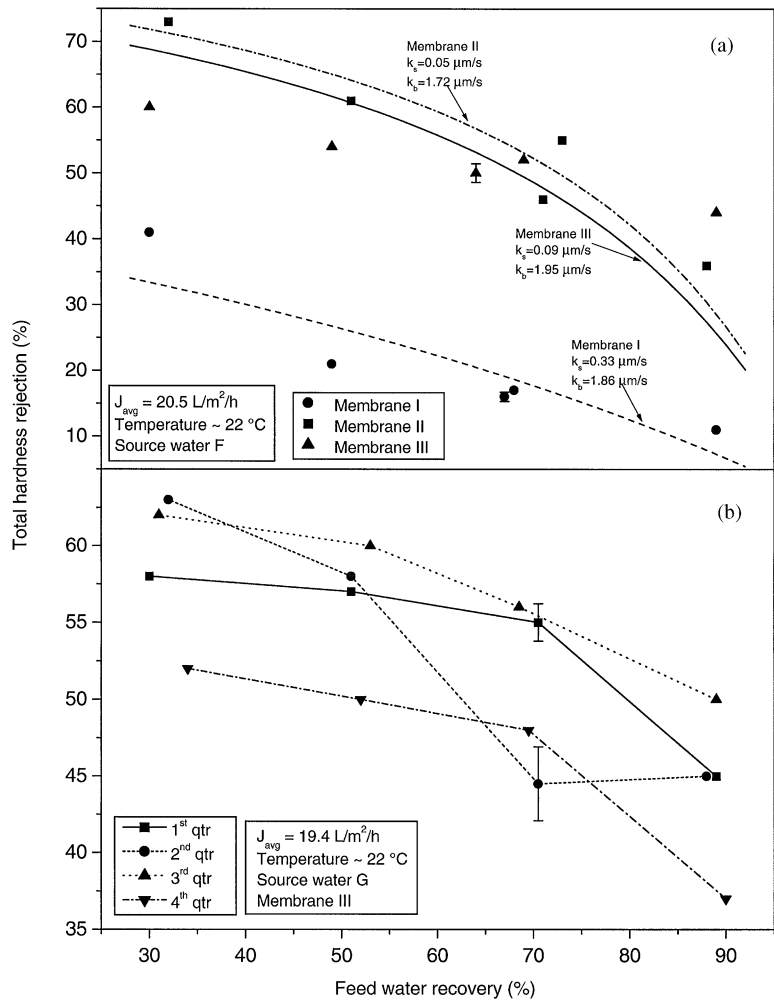


Fig. 5. Comparison of total hardness rejection by three NF membranes at various feed-water recoveries for source water F (a). Theoretical fits are superposed (along with model parameters) on experimental observations for comparison. Total hardness rejection for replicate experiments conducted over four quarters with seasonal variations in source water G water quality using membrane III are shown in (b).

$\mu\text{m/s}$) for the first quarter of testing are shown in Fig. 7(e) in the range $0 \leq k_s \leq 0.25 \text{ } \mu\text{m/s}$ and $0.8 \leq k_b \leq 12.4 \text{ } \mu\text{m/s}$ along with profile traces of \hat{k}_s on k_b and \hat{k}_b on k_s . As seen in Fig. 7(e), the likelihood regions are extremely large and remain divergent even as k_s and k_b are increased to 10 and six times their least-squares estimate, respectively. The lower bounds for the 95% joint likelihood intervals for k_s and k_b can be read directly off Fig. 7(e) as ~ 0 and $0.80 \text{ } \mu\text{m/s}$, respectively. The upper bounds for significance levels $> 50\%$ cannot be estimated because the likelihood contours do not close. Profile traces of \hat{k}_b on k_s and \hat{k}_s on k_b are coincident in the range shown and curved over a wide range of parameter values indicating that the contours are long, tapering and markedly non-elliptical. This behavior again reveals the inherent severe non-linearity of the model-data set combination collected under the ICR protocol.

Similar diagnostics of least-square estimates for other inorganic and organic contaminant rejection

for various source water membrane combinations were observed (data not shown). All profile t plots were highly skewed and showed asymptotic behavior indicative of highly non-linear behavior with poor precision suggesting that the design of bench-scale NF experiments under the ICR could be improved. Fig. 7(f) shows joint likelihood regions of k_s and k_b obtained by pooling data from four quarters of experiments conducted at the four EPA mandated recovery values (30, 50, 70, and 90%). Increasing the degrees of freedom from 3 to 18 by pooling data resulted in 50 and 75% nominal contours to close on both sides of the point estimate. However, the 95% joint likelihood contour remained open to the right (unbounded upper limit). Thus, increasing the number of observations alone leads to greater precision. One method of collecting more data for a set of experiments under the ICR without changing the financial burden on the affected utilities could have been to halve the number of seasonal

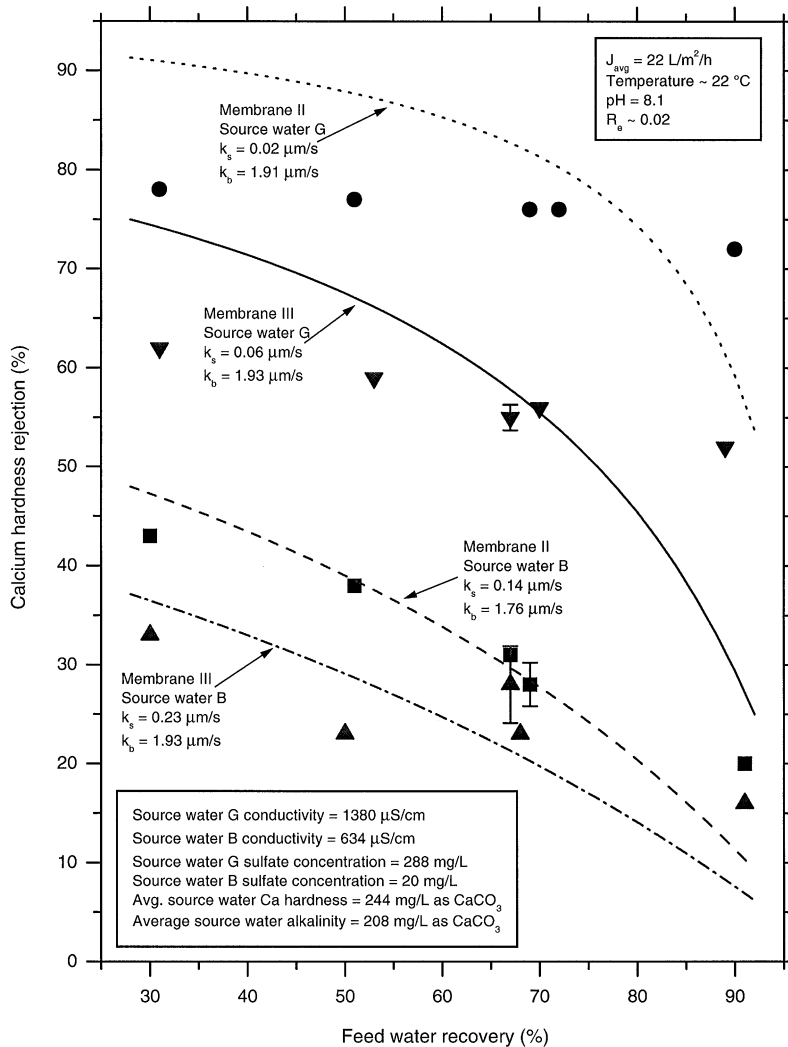


Fig. 6. Evidence of coupling between calcium and sulfate ion transport across membranes II and III. Note that calcium rejection increased by a factor of ~ 2 at all recoveries for a ~ 14 fold increase in feed water SO_4^{2-} concentration.

evaluations to 2 while doubling the number of required samples. Additionally, more prudently choosing recovery values could have also lead to increased precision of parameter estimates. As expected, the profile traces intersect the sum of squares of surface where the contours have horizontal or vertical tangents (Watts, 1994).

MODEL APPLICATION

Figures 2–7 depict good model fits to experimental data (when coupling is small) in terms of contaminant rejection. However, drinking water MCLs for most inorganic and organic chemicals are based on absolute concentrations rather than percent removal. Hence, the potential for NF to meet regulations is inherently dependent on membrane feed water concentrations. One method of employing the model

(equation (10)) is shown in Fig. 8 which depicts constant permeate concentration surfaces using k_s and k_b values estimated for source water G and membrane III. TTHM and HAA9 precursor surfaces corresponding to 80 and 60 $\mu\text{g/L}$ (loosely based on USEPA's Stage I D/DBP rule) as well as 40 and 30 $\mu\text{g/L}$ (based on Stage II D/DBP rule placeholders) are shown in Fig. 8(a) and (b), respectively. (The chosen permeate concentrations could be a regulatory MCL or a more stringent level determined by individual utilities based on greater public health protection.) These surfaces show maximum feed water concentrations of TTHM and HAA9 precursors that can be effectively treated by this membrane for various combinations of flux and recovery. Thus, at 20 $\text{L/m}^2/\text{h}$ flux and 70% recovery, anticipated Stage II MCLs will be achieved only when feed water concentrations are $< \sim 330 \mu\text{g/L}$ for TTHM precursors (point A1 in Fig. 8(a)) and $< \sim 250 \mu\text{g/L}$ for

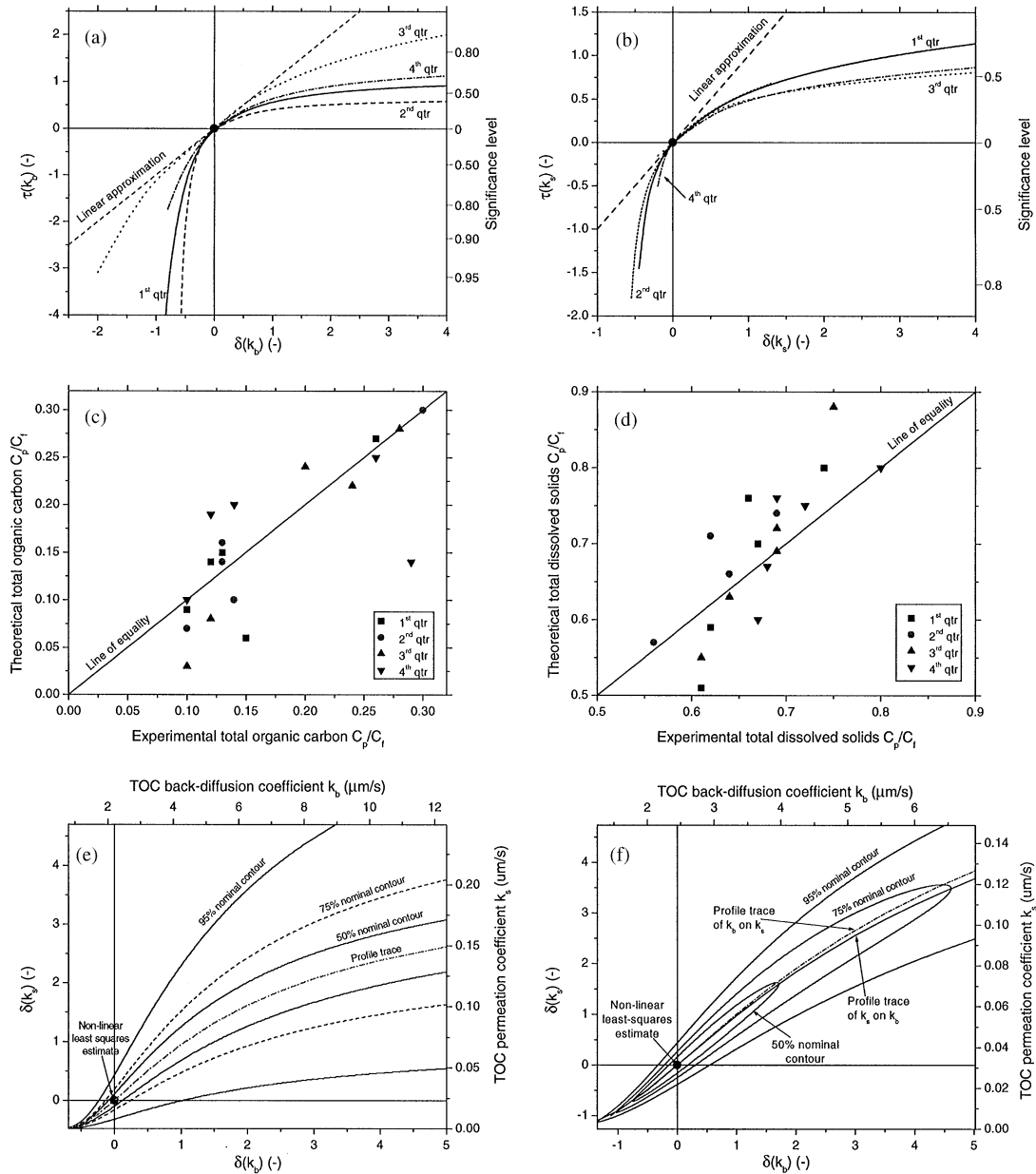


Fig. 7. Summary of non-linear statistical parameter estimation for four quarters of contaminant removal from source water G using membrane III. Profile t plots for TOC k_b and k_s are depicted in (a) and (b) respectively, along with the linear approximation. Comparison of experimental data and theoretical calculations according to equation (10) for each quarter are shown in (c) and (d) for TOC and total dissolved solids, respectively. Profile traces, 50, 75, and 95% joint likelihood regions for the first quarter TOC data are given in (e) where the joint likelihood regions do not close on the right (indeterminable upper confidence limit) and the profile traces of k_s on k_b and k_b on k_s are coincident. Point estimates of k_s and k_b derived by non-linear regression after pooling all four quarters of TOC data are given in (f) where 50 and 75% joint likelihood regions are seen to close and the profile traces are not coincident.

HAA9 precursors (point A2 in Fig. 8(b)), respectively if free chlorine is employed. Because transport of DBP precursors across these NF membranes are limited by molecular diffusion, compliance with anticipated Stage II regulations using membrane III will be possible only when feed water concentrations decrease to below $\sim 140 \mu\text{g/L}$ for both TTHM and

HAA9 precursors at $40 \text{ L/m}^2/\text{h}$ flux and 90% recovery if free chlorine is employed.

These results again demonstrate the increased importance of recovery over flux on permeate water quality. Similar plots can be made for other membrane–source water combinations (and other contaminants) to better interpret water quality data

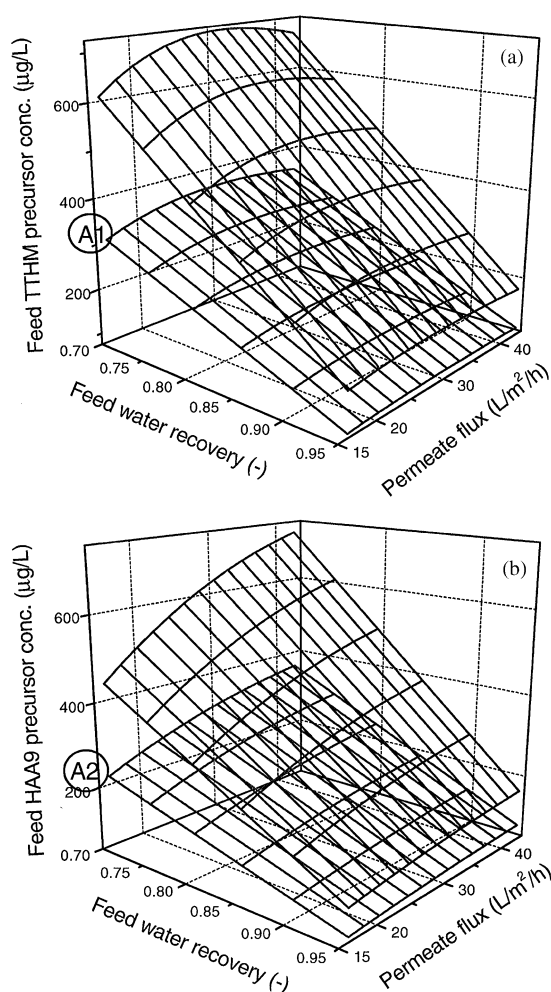


Fig. 8. Constant TTHM (a) and HAA9 (b) permeate concentration surfaces. Mass transfer coefficients correspond to those calculated for source water G and membrane III (TTHM $k_s=0.123$, TTHM $k_b=8.75$; HAA9 $k_s=0.166$, HAA9 $k_b=17.72 \mu\text{m/s}$). Surfaces loosely correspond to Stage I MCLs (80/60 $\mu\text{g/L}$) and Stage II placeholders (40/30 $\mu\text{g/L}$) of USEPA's D/DBP rule and depict the maximum feed concentration that can be effectively treated to reduce TTHM and HAA9 precursors to these regulatory levels.

obtained with changing operating conditions in pilot-scale experiments conducted in support of plant design. Thus, the design flux and recovery may be controlled by permeate water quality and/or fouling. This approach also allows plant operators or automatic control systems to adjust flux/recovery to comply with MCLs of diffusion-limited contaminants with changes in the feed water quality.

CONCLUSIONS

Nonlinear fits of mass transfer coefficients to a simple closed-form analytical expression suggests that the design of bench-scale NF treatment studies

mandated under USEPA's information collection rule could be improved to obtain greater precision of these parameters. Increasing the number and location of recovery values is expected to increase the precision of parameter estimates. Our approach to rejection calculations cannot be employed in a purely predictive mode for a multi-component system primarily because fundamental thermodynamic properties of contaminants encountered in water treatment have not yet been determined due to their heterogeneity as well as the complex composition of natural and pretreated feed waters. This is not surprising because, even mass transfer coefficients of single, fully dissociated ionic solutions are dependent on solute concentration (Eriksson, 1988) and are difficult to predict a priori. Complexation of inorganic ions with NOM, incomplete characterization of membrane and feed water composition, and unavailability of methods to identify dominant ion pairs encountered in water treatment (Marinas and Selleck, 1992) can be expected to further complicate rejection calculations from multi-solute solutions.

Coupled transport of divalent inorganic ions across negatively charged membranes further confounded rejection calculations. For example, increasing SO_4^{2-} concentrations increased Ca^{+2} rejection while decreasing alkalinity rejection. Hence, care should be taken before universalizing softening and alkalinity removal capabilities of membranes without considering the complete feed water chemistry. These results underscore the continued need for site-specific studies for water quality evaluations in addition to determining fouling rates and other plant design parameters.

Even with these limitations, the simplified model can quantitatively fit rejection of NOM, DBP precursors, and inorganic contaminants (when coupling is low) by various TFC-NF membranes. This result is consistent with the notion that molecular diffusion plays an important role in contaminant rejection even in NF membranes under conditions typical of water treatment. The model can also be employed to better interpret site-specific bench-, and pilot-scale experiments conducted in support of plant design. For example, our calculations suggest that flux will have a lower impact on permeate water quality compared to recovery. However, NF fouling rate is a strong function of permeate flux (Chellam *et al.*, 1997). Hence, pilot-scale experiments should be conducted at various fluxes primarily to determine design values during which time water quality sampling can be reduced in order to decrease project cost. Diffusion-dominated transport of NOM and DBP precursors may limit the upper bound of recovery and/or necessitate changes in the secondary disinfectant for highly colored waters to comply with anticipated Stage II DBP regulations. Thus, the design recovery in installations employing these new generation NF membranes in water treatment should be determined from considerations of concentrate

disposal, precipitative fouling, as well as finished water quality.

Acknowledgements—Gerry Filteau, Stuart McClellan, Terry Smith, Tom Stocker, and Mark Wilf provided membrane samples. Jennifer Abrajano, Daniel Bush, Paige Igoe, Joseph Jacangelo, Eric Landsberg, Jason Radgowski, and David Wilkes assisted in the conduct of experiments. The comments of Srinivas Veerapaneni and two anonymous reviewers are greatly appreciated, as are useful discussions with Ramesh Sharma. This work was partially supported by a grant from the Texas Water Resources Institute and the United States Geological Survey (Grant # 144000-5224).

REFERENCES

- Allgeier S. C. and Summers R. S. (1995) Evaluating NF for DBP control with the RBSMT. *J. Am. Water Works Assoc.* **87**(3), 87–99.
- Amy G. L., Collins M. R., Kuo C. J. and King P. H. (1987) Comparing gel permeation chromatography and ultrafiltration for the molecular weight characterization of aquatic organic matter. *J. Am. Water Works Assoc.* **79**(1), 43–49.
- Bates D. M. and Watts D. G. (1988) *Nonlinear Regression Analysis and Its Applications*. Wiley, New York, N.Y.
- Blau T. J., Taylor J. S., Morris K. E. and Mulford L. A. (1992) DBP control by nanofiltration: cost and performance. *J. Am. Water Works Assoc.* **84**(12), 104–116.
- Chellam S. (2000) Effects of nanofiltration on trihalo-methane and haloacetic acid precursor removal and speciation in waters containing low concentrations of bromide ion. *Environ. Sci. Technol.* **34**(9), 1813–1820.
- Chellam S., Jacangelo J. G., Bonacquisti T. P. and Schauer B. A. (1997) Effect of pretreatment on surface water nanofiltration. *J. Am. Water Works Assoc.* **89**(10), 77–89.
- Childress A. E. and Elimelech M. (1996) Effect of solution chemistry on the surface charge of polymeric reverse osmosis and nanofiltration membranes. *J. Memb. Sci.* **119**, 253–268.
- Chin Y.-P., Aiken G. and O'Loughlin E. (1994) Molecular weight, polydispersivity, and spectroscopic properties of aquatic humic substances. *Environ. Sci. Technol.* **28**(11), 1853–1858.
- Cho J., Amy G. L. and Pellegrino J. (1999) Membrane filtration of natural organic matter: Initial comparison of rejection and flux decline characteristics with ultrafiltration and nanofiltration membranes. *Water Res.* **33**(11), 2517–2526.
- Clesceri L. S., Greenberg A. E. and Eaton A. D. eds. (1998) *Standard methods for the examination of water and wastewater*. 20th Ed. on American Public Health Association, Washington DC.
- Croue J. P., Debroux J. F., Amy G. L., Aiken G. R. and Leenheer J. A. (1999) Natural organic matter: structural characteristics and reactive properties. *Formation and Control of Disinfection By-Products in Drinking Water*, ed P. C. Singer, pp. 65–93. AWWA: Denver, CO.
- Dennis J. E., Gay D. M. and Welsch R. E. (1981) An adaptive nonlinear least-squares algorithm. *ACM Trans. Math. Soft.* **7**(3), 348–368.
- Eriksson P. (1988) Water and salt transport through two types of polyamide composite membranes. *J. Memb. Sci.* **36**, 297–313.
- Hong S. and Elimelech M. (1997) Chemical and physical aspects of natural organic matter fouling of nanofiltration membranes. *J. Memb. Sci.* **132**, 159–181.
- Jonsson G. and Boesen C. E. (1984) Polarization phenomena in membrane processes. In *Synthetic Membrane Processes: Fundamentals and Water Applications*, ed G. Belfort, pp. 101–130. Academic Press, New York, NY.
- Lonsdale H. K. (1979) Theory and practice of reverse osmosis and ultrafiltration. In *Industrial Processing with Membranes*, eds R. E. Lacey and S. Loeb, pp. 123–178. Robert E. Krieger Publishing Company: Huntington, NY.
- Lonsdale H. K., Merten U. and Riley R. L. (1965) Transport properties of cellulose acetate osmotic membranes. *J. Appl. Poly. Sci.* **9**, 1341–1362.
- Marinas B. J. and Selleck R. E. (1992) Reverse osmosis treatment of multicomponent electrolyte solutions. *J. Memb. Sci.* **72**, 211–229.
- Martell A. E. and Motekaitis R. J. (1992) *Determination and Use of Stability Constants*. VCH Publishers, New York, NY.
- Matsuura T. (1993) *Synthetic Membranes and Membrane Separation Processes*. CRC Press, Boca Raton, FL.
- Press W. H., Teukolsky S. A., Vetterling W. T. and Flannery B. P. (1992) *Numerical Recipes in FORTRAN: The Art of Scientific Computing*. Cambridge University Press, New York, NY.
- Rosa M. J. and de Pinho M. N. (1994) Separation of organic solutes by membrane pressure-driven processes. *J. Memb. Sci.* **89**, 235–243.
- Soltanieh M. and Gill W. N. (1981) Review of reverse osmosis membranes and transport models. *Chem. Engng. Commun.* **12**, 279–363.
- Sourirajan S. (1970) *Reverse Osmosis*. Academic Press, New York, NY.
- Stumm W. J. and Morgan J. (1996) *Aquatic Chemistry: Chemical Equilibria and Rates in Natural Waters*. Wiley, New York, NY.
- Tan L. and Amy G. L. (1991) Comparing ozonation and membrane separation for color removal and disinfection by-product control. *J. Am. Water Wks. Assoc.* **83**(5), 74–79.
- Taylor J. S. and Jacobs E. P. (1996) Reverse osmosis and nanofiltration. In *Water Treatment Membrane Processes*, eds J. Mallevalle, P. E. Odendaal and M. R. Wiesner, pp. 9.1–9.70. McGraw Hill, New York, NY.
- USEPA (1996) ICR manual for bench- and pilot-scale treatment studies. Office of Ground Water and Drinking Water: Cincinnati, OH, USA, pp. 1-1–3-108 (EPA 814-B-96-003).
- USEPA (1998) National primary drinking water regulations: Disinfectants and disinfection by-products; final rule, pp. 69 390–69 476. Washington DC.
- van den Berg G. B., Racz I. G. and Smolders C. A. (1989) Mass transfer coefficients in ultrafiltration. *J. Memb. Sci.* **47**, 25–51.
- van der Bruggen B., Schaer J., Wilms D. and Vandecasteele C. (1999) Influence of molecular size, polarity, and charge on the retention of organic molecules by nanofiltration. *J. Memb. Sci.* **156**, 29–41.
- Watts D. G. (1994) Estimating parameters in non-linear rate equations. *The Can. J. Chem. Engng.* **72**, 701–710.
- Wiesner M. R. and Buckley C. A. (1996) Principles of rejection in pressure-driven membrane processes. In *Water Treatment Membrane Processes*, eds J. Mallevalle, P. E. Odendaal and M. R. Wiesner, pp. 5.1–5.17. McGraw Hill, New York, NY.